AGU PUBLICATIONS

Paleoceanography and Paleoclimatology

RESEARCH ARTICLE
10.1002/2017PA003238

Key Points:
- Long-term decrease in neodymium isotope ratios from fossil fish teeth reflects increased export of northern component water to proto-CDW
- Record from ODP Site 744 suggests a local response to glacial weathering of Antarctica
- Neodymium isotope ratios from Kerguelen Plateau show no change in water mass mixing related to the Drake Passage

Supporting Information:
- Supporting Information S1

Correspondence to:
N. M. Wright,
nicky.wright@sydney.edu.au

Citation:
Wright, N. M., Scher, H. D., Seton, M., Huck, C. E., & Duggan, B. D. (2018). No change in Southern Ocean circulation in the Indian Ocean from the Eocene through late Oligocene. *Paleoceanography and Paleoclimatology*, *33*, 152–167. https://doi.org/10.1002/2017PA003238

Received 5 SEP 2017
Accepted 20 DEC 2017
Accepted article online 3 JAN 2018
Published online 5 FEB 2018

No Change in Southern Ocean Circulation in the Indian Ocean From the Eocene Through Late Oligocene

Nicky M. Wright[1], Howie D. Scher[2], Maria Seton[1], Claire E. Huck[3], and Brian D. Duggan[2]

[1]EarthByte Group, School of Geosciences, University of Sydney, Sydney, New South Wales, Australia, [2]Department of Earth and Ocean Sciences, University of South Carolina, Columbia, SC, USA, [3]Department of Ocean and Earth Science, National Oceanography Centre, University of Southampton, Southampton, UK

Abstract Deciphering the evolution of Southern Ocean circulation during the Eocene and Oligocene has important implications for understanding the development of the Antarctic Circumpolar Current and transition to Earth's "icehouse" climate. To better understand ocean circulation patterns in the Indian Ocean sector of the Southern Ocean, we generated a new fossil fish tooth neodymium isotope record (ε_{Nd}) from the upper Eocene to upper Oligocene sections (36–23 Ma) of Ocean Drilling Program Sites 744 and 748 (Kerguelen Plateau, Indian Ocean). Reconstructed seawater ε_{Nd} values from fossil fish teeth are used to trace changes in water masses across ocean basins. The records from Site 748 and Site 744 reveal a gradual shift from ε_{Nd} values around −6.5 to −7.5 in the late Eocene to ε_{Nd} values between −7.5 and −8.3 by the late Oligocene, consistent with a Circumpolar Deep Water (CDW) influence at the Kerguelen Plateau throughout the Oligocene. We interpret the shift to less radiogenic values to reflect the increased export of Northern Component Water to the Southern Ocean, likely into the proto-CDW. However, the records show no major change in water mass composition around the Kerguelen Plateau that would accompany an increase in Pacific throughflow related to the opening of Drake Passage and imply that Pacific throughflow via the Drake Passage occurred by the late Eocene. High-frequency variability in ε_{Nd} values at Site 744 is interpreted as an imprint of Oligocene glacial activity, with a particularly pronounced excursion at 32.6 Ma roughly coinciding with other glacial weathering indicators around Antarctica.

1. Introduction

The evolution of ocean circulation patterns in the Southern Ocean during the Cenozoic is not fully understood, especially during critical climatic events such as the onset of significant Antarctic glaciation at the Eocene-Oligocene transition (EOT; ~34 Ma; e.g., Miller et al., 1987; Zachos et al., 1996, 2001). Ocean circulation is responsible for heat transport, and it has been proposed that the tectonic opening of Southern Ocean gateways (i.e., the Tasman Gateway and Drake Passage) allowed for a reorganization in ocean circulation, including the onset of the Antarctic Circumpolar Current (ACC), ultimately resulting in the thermal isolation of Antarctica and significant glaciation across the EOT (e.g., Kennett, 1977). Neodymium (Nd) isotope ratios can be employed as a proxy for reconstructing ocean circulation patterns and have been used to identify the inception of the ACC at around 30 Ma, linking the onset of the ACC to the opening and migration of the Tasman gateway into the westerly wind band (Scher et al., 2015). However, the role of the Drake Passage in the development of the ACC is unclear due to uncertainties in the timing of deep gateway opening and the paleobathymetric evolution of the Scotia Sea. Neodymium isotope ratios from the Atlantic sector of the Southern Ocean suggest an influx of Pacific seawater through the Drake Passage as early as 41 Ma (Scher & Martin, 2006). This age predates the earlier estimates of deep Scotia Sea gateway opening (e.g., 23 Ma; Barker & Burrell, 1977); however, recent studies suggest the establishment of a deep water connection through the Drake Passage from 34–30 Ma (Eagles & Jokat, 2014; Livermore et al., 2005, 2007) to ~12 Ma (Dalziel et al., 2013).

While previous work on reconstructing ocean circulation patterns around the Eocene-Oligocene boundary has largely focused on the South Atlantic (e.g., Scher & Martin, 2004, 2006, 2008; Via & Thomas, 2006) and the Tasman Gateway (Scher et al., 2015), comparatively little work has been published on pathways through the Indian Ocean. This has presented a challenge for explaining similarities in isotope records between Maud Rise (Atlantic sector), East Tasman Plateau (Tasman Sea sector), and Hikurangi Plateau (Pacific sector)—which

suggest water mass communication between these regions. An additional motivation for constructing long Nd isotope records on Kerguelen Plateau is to explore the influence that this large topographic barrier has on the flow of the modern ACC. The Kerguelen Plateau, a shallow submarine plateau in the Indian sector of the Southern Ocean, forms a critical obstacle for the ACC and diverts most ACC transport to the north of the barrier (Park et al., 1993). Such bathymetric highs likely influenced the pathway of the ACC during the Cenozoic (e.g., Munday et al., 2015).

Here we fill the gap in the Indian Ocean using Nd isotope ratios extracted from fossil fish teeth to reconstruct the composition of ancient seawater in the high latitude Indian Ocean. We present Nd isotope records from the upper Eocene to upper Oligocene sections of Ocean Drilling Program (ODP) Sites 744 (Leg 119) and 748 (Leg 120) located on the Kerguelen Plateau (Figure 1). The Kerguelen Plateau is immediately downstream from the Weddell Sea, and proximal to Cape Darnley in Prydz Bay, which are both sources of bottom water today. We explore the origins of Nd isotope variability in our new records by comparison to existing Nd isotope data sets from the Indian, Atlantic, and Pacific sectors of the Southern Ocean (Figure 1a). We then use our record to explore the evolution of Southern Ocean circulation during the Eocene and Oligocene and assess these results in terms of Cenozoic climate and Antarctic glaciation patterns.

1.1. The Use of Neodymium Isotopes as a Tracer for Circulation Patterns

The Nd isotopic composition of fossil fish teeth from pelagic marine environments can be used as a proxy for reconstructing water mass circulation patterns. The ε_{Nd} value of fossil fish teeth (where $\varepsilon_{Nd} = [(^{143}Nd/^{144}Nd)_{measured}/(^{143}Nd/^{144}Nd)_{CHUR}] - 1 \times 10^4$, where CHUR is the Chronditic Uniform Reservoir with $^{143}Nd/^{144}Nd = 0.512638$ (Jacobsen & Wasserburg, 1980)) reflects the Nd isotopic composition of seawater in contact with the seafloor at the time of deposition, remineralization, and burial of fish teeth (Staudigel et al., 1985). The ε_{Nd} value of fossil fish teeth from deep-sea sediment cores is resistant to postburial alteration (Martin & Haley, 2000; Scher et al., 2011), making fossil fish teeth a faithful archive for bottom water ε_{Nd} values at the time of deposition. Due to short residence time of Nd in the ocean (~300–1,000 years) (Arsouze et al., 2009; Rempfer et al., 2011; Tachikawa et al., 2003), ε_{Nd} records from fossil fish teeth can be used to reconstruct past ocean circulation patterns.

Neodymium is introduced into the ocean through the erosion of continental sources, such as dissolved riverine input, dust transport, and by exchange with sediments on continental margins known as boundary exchange (Allègre et al., 2010; Frank, 2002; Lacan & Jeandel, 2005a, 2005b; Piepgras & Wasserburg, 1980). The Nd isotopic composition of continental crust largely reflects its age and type. During melt extraction from the mantle, samarium (Sm) has a greater compatibility than Nd, resulting in higher Sm/Nd in the mantle relative to the crust (Jacobsen & Wasserburg, 1980). Due to the decay of radioactive ^{147}Sm to ^{143}Nd over time, older granitic cratons develop extremely negative ε_{Nd} values, whereas young volcanic outcrops are more positive (Goldstein & Hemming, 2003; Jeandel et al., 2007). Thus, water masses originating from regions where young volcanogenic derived material is weathered have more positive (radiogenic) ε_{Nd} values (e.g., Pacific Ocean; $\varepsilon_{Nd} = 0$ to -5; Goldstein & Hemming, 2003), while contributions from ancient continental rocks result in more negative (unradiogenic) values, in basins such as the North Atlantic (e.g., North Atlantic Deep Water, NADW; $\varepsilon_{Nd} = -13.6 \pm 0.5$; Lambelet et al., 2016). Neodymium isotope ratios are not influenced by biological fractionation, weathering, or transport processes (Goldstein & Hemming, 2003; Lacan & Jeandel, 2001); therefore, variations in the ε_{Nd} value of a water mass reflect mixing with other water bodies and/or contact and exchange with continental inputs.

2. Regional Setting and Hydrography

2.1. Geologic Setting of the Kerguelen Plateau

ODP Site 744, Hole 744A (61.579°S, 80.595°E; water depth: 2307.3 m) and Site 748, Hole 748B (58.441°S, 78.9981°E; water depth: 1290.9 m) are positioned on the southern domain of the Kerguelen Plateau (Figure 1), a large igneous province (LIP) presently located on the Antarctic plate. It is bound by the Enderby Basin to its southwest, the Crozet Basin to its northwest, and the Australian-Antarctic Basin to its northeast and is separated from the Antarctic continent by the Princess Elizabeth Trough. The Kerguelen Plateau can be divided into distinct domains, including the southern Kerguelen Plateau, central Kerguelen Plateau, northern Kerguelen Plateau, Elan Bank, and the Labuan Basin (Figure 1b).

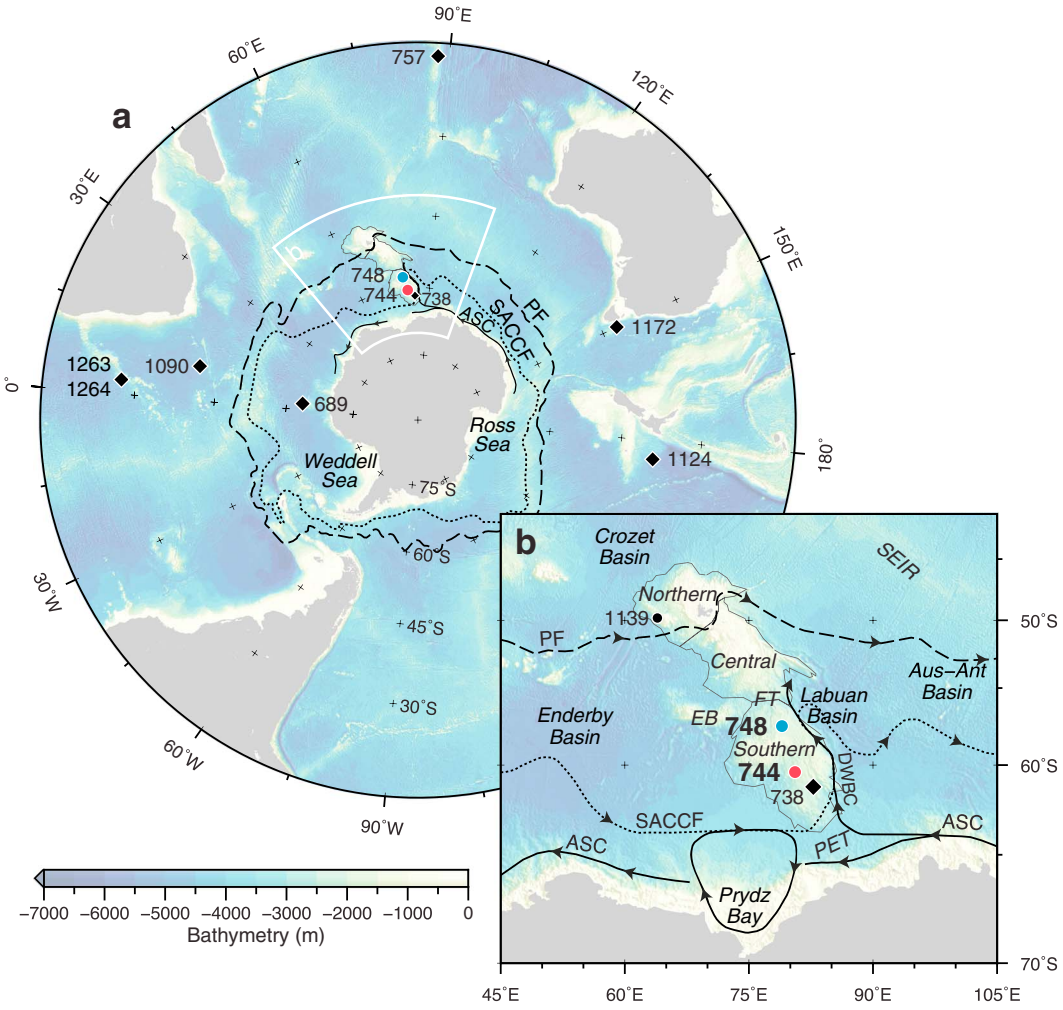

Figure 1. (a) Overview of the present-day Southern Ocean and study sites (ODP Sites 744 and 748) (circles) and ODP sites (diamonds) considered in this study. (b) Map of the Kerguelen Plateau and study sites. Bathymetry (ETOPO1; Amante & Eakins, 2009), present-day coastlines (light gray), and the Kerguelen Plateau (thin gray outline; from Whittaker et al., 2015) are shown. Fronts and currents shown include Antarctic slope current (ASC; based on McCartney & Donohue, 2007, and Roquet et al., 2009), Deep Western Boundary Current (DWBC; based on Park et al., 2008, and Roquet et al., 2009); Polar Front (PF; from Orsi et al., 1995, modified around Kerguelen Plateau based on Park et al., 2008, and Roquet et al., 2009); Pyrdz Bay Gyre (modified from Borchers et al., 2011); Southern Antarctic Circumpolar Current Front (SACCF; from Orsi et al., 1995). ODP Leg 183, Site 1139 (Skiff Bank) is shown for its location only. Abbreviations are Aus-Ant Basin, Australian-Antarctica Basin; EB, Elan Bank; FT, Fawn Trough; PET, Princess Elizabeth Trough; SEIR, Southeast Indian Ridge.

The Kerguelen Plateau formed from volcanic activity associated with the Kerguelen plume, with emplacement of the Kerguelen Plateau occurring since the Cretaceous. Eruption ages decrease northward across the Kerguelen Plateau: ages from southern Kerguelen Plateau basalts are 118–110 Ma (Coffin et al., 2002; Duncan, 2002), central Kerguelen Plateau basalts are 100–95 Ma (Duncan, 2002), and northern Kerguelen Plateau ages are 40–35 Ma (Duncan, 2002). While the central and northern Kerguelen Plateaus are composed of volcanic material related to ridge-plume interactions, continental fragments found within the crust of the southern Kerguelen Plateau suggest that this plateau is at least partially underlain by stretched continental crust (Bénard et al., 2010). The uppermost crust of the Kerguelen Plateau was largely emplaced subaerially, based on vesicularity and oxidative alteration of basalts recovered from ODP cores (Coffin et al., 2002; Duncan, 2002; Frey et al., 2000).

Volcanic activity associated with southern Kerguelen Plateau eruption predates our study period; however, emplacement of the northern Kerguelen Plateau coincides with the timing of our Nd isotope record. The northern Kerguelen Plateau formed from ~40 Ma, based on basalts recovered from Leg 183, Site 1140 (Duncan, 2002), although a date of ~68 Ma has been obtained from ODP Leg 183, Site 1139 (Skiff Bank)

(Duncan, 2002), where Skiff Bank constitutes ~10% of northern Kerguelen Plateau (Coffin et al., 2002). Basalts from Skiff Bank are similar to those from the northern Kerguelen Plateau (Frey et al., 2003), and its older age may be due to overprinting at Site 1139 (Duncan, 2002) or may reflect an earlier emplacement age for portions of the northern Kerguelen Plateau (Duncan, 2002). After emplacement at 40 Ma, volcanic activity moved progressively southward and possibly represents the hot spot track of the Kerguelen plume (Weis et al., 2002), with activity at the presently subaerial Kerguelen archipelago around 30–24 Ma (Nicolaysen et al., 2000), to recent volcanic activity on Heard Island (Weis et al., 2002). Subaerial emplacement is inferred from Skiff Bank (Site 1139) (Frey et al., 2000); however, basaltic pillow lavas recovered from Site 1140 suggest submarine emplacement corresponding with major northern Kerguelen Plateau emplacement, with an 870 m paleodepth estimate (Wallace, 2002).

2.2. Southern Ocean Circulation

2.2.1. Present Day

The present-day Kerguelen Plateau has a major influence on both regional circulation and the fronts of the ACC, where it forms the largest topographic obstacle to circumpolar flow (Sokolov & Rintoul, 2009). The southern Kerguelen Plateau is largely under the influence of Circumpolar Deep Water (CDW), which is the most voluminous Southern Ocean water mass and encompasses most of the deep ocean between the northerly polar front (PF) and Southern Antarctic Circumpolar Current Front (SACCF) (Figure 1) (Orsi et al., 1995). The PF passes by the north of northern Kerguelen Plateau (e.g., Belkin & Gordon, 1996; Orsi et al., 1995), while the SACCF passes through the Princess Elizabeth Trough, located immediately south of southern Kerguelen Plateau (McCartney & Donohue, 2007; Orsi et al., 1995; Roquet et al., 2009) (Figure 1). Detailed regional studies have debated the precise pathway of these fronts around Kerguelen Plateau (e.g., Park et al., 1998, 2008, 2009; Roquet et al., 2009); however, southern Kerguelen Plateau is dominated by CDW regardless of the slight variations in PF and SACCF locations.

After the SACCF passes through the Princess Elizabeth Trough, it bends steeply northwestward to form part of the deep western boundary current (DWBC) along the eastern flank of southern Kerguelen Plateau (McCartney & Donohue, 2007; Roquet et al., 2009). The Kerguelen DWBC (Figure 1) is a strong geostrophic current and the main source of water to the Southern Kerguelen Plateau, transporting cold deep water (including Antarctic Bottom Water; AABW) and suspended sediment away from the Antarctic margin (Donohue et al., 1999; Fukamachi et al., 2010). This current forms the western limb of a cyclonic gyre in the Australian-Antarctic basin (McCartney & Donohue, 2007; Park et al., 2009). Sources for the Kerguelen DWBC include (1) the westward flow of the Antarctic Slope Current (or Front; ASC), which transports AABW from the Adélie Coast/Wilkes Land Basin (Donohue et al., 1999; Fukamachi et al., 2010), and the Ross Sea (Fukamachi et al., 2010) to the DWBC (McCartney & Donohue, 2007); and (2) the eastward flow of AABW from the Weddell-Enderby Basin, which is entrained within the ACC (Donohue et al., 1999; Heywood et al., 1999; McCartney & Donohue, 2007) and passes the continental shelf adjacent to Prydz Bay to also bring terrigenous material from Prydz Bay through the Princess Elizabeth Trough to the DWBC (Borchers et al., 2011). Recent work has also suggested that dense shelf water produced in Cape Darnley, located on the western side of Prydz Bay, contributes to AABW (Ohshima et al., 2013; Williams et al., 2016; Yabuki et al., 2006). South of the Kerguelen Plateau, the cyclonic Prydz Bay Gyre (Figure 1) mixes and recirculates waters from the ASC and AABW with CDW (Heywood et al., 1999; Nunes Vaz & Lennon, 1996; Smith et al., 1984), along with terrigenous material from Prydz Bay (Borchers et al., 2011).

Circumpolar Deep Water is predominately influenced by NADW, where 70–75% of the CDW Nd budget is contributed by NADW (Stichel et al., 2012). The average modern ε_{Nd} value for CDW is −8.5 (Stichel et al., 2012) and is more radiogenic than modified NADW (ε_{Nd} = −10 to −11; Stichel et al., 2012) and "true" NADW (ε_{Nd} = −13.6; Lambelet et al., 2016). Average ε_{Nd} for modern AABW varies depending on its source; AABW derived from the Ross Sea is ε_{Nd} = −7 (Rickli et al., 2014), from the Weddell Sea is ε_{Nd} = −8.9 (Stichel et al., 2012), and is inferred from ferromanganese crust measurements for the Adélie Coast/Wilkes Land Basin to be around ε_{Nd} = −10 (van de Flierdt et al., 2006).

2.2.2. Eocene and Oligocene

The Paleogene Southern Ocean had many differences compared to its modern expression. During the Paleocene-early Eocene, the Southern Ocean was likely dominated by deep waters forming in locations similar to the modern day (e.g., Huck et al., 2017; Thomas et al., 2003), with limited contribution of deep water

from the North Atlantic. Export of an early expression of Northern Component Water (NCW), the ancient precursor to NADW, to the midlatitude North Atlantic basin from 38.5 Ma has been proposed by Borrelli et al. (2014) based on benthic foraminiferal stable isotopes. A later onset of NCW export has been linked to the deepening of the Greenland-Scotland Ridge by the early Oligocene (Abelson et al., 2008; Davies et al., 2001; Via & Thomas, 2006). However, it is not clear if these waters contributed to proto-CDW in the Southern Ocean during the late Eocene. More recognizable features of Southern Ocean circulation and modern climate evolved around the EOT. Major stepwise cooling has been inferred from magnesium/calcium (Mg/Ca) records from planktonic foraminifera from ODP Sites 738, 744, and 748 (southern Kerguelen Plateau) (Bohaty et al., 2012). Other major changes across the EOT include higher ocean productivity (Diester-Haass & Zahn, 2001), high-latitude cooling of ocean surface waters (Liu et al., 2009), and the large-scale growth of permanent ice sheets on Antarctica (Lear et al., 2000; Miller et al., 1987). These changes were likely precipitated from the organization of the Southern Ocean frontal zones. The formation of a proto-PF and protosubtropical fronts may have occurred by the middle to late Eocene (~42 Ma), based on the presence of bolboforms (an extinct group of microplankton), variations of planktonic foraminiferal diversity, and the presence of ice rafted debris (IRD) in Site 748 (Cooke et al., 2002). These proto oceanic fronts formed poleward (proto-PF: <~70–60°S; proto-STF: 65–50°S) of their present-day positions (PF: ~60–50°S; STF: 30–40°S) and progressed equatorward during the Oligocene and Miocene (Cooke et al., 2002). Fully coupled climate models for the Eocene indicate subtropical and subpolar gyres, including a clockwise subpolar gyre passing north of Kerguelen Plateau and with westward flow through Princess Elizabeth Trough (Huber et al., 2004).

Despite the uncertainties and differences in ocean circulation between our study period (36–23 Ma; late Eocene to Oligocene) and the modern day, water masses and transport pathways around the southern Kerguelen Plateau are thought to have been similar to present day (e.g., Kerguelen DWBC; Scher et al., 2014), which are predominantly driven by the pressure gradient force exerted on the Kerguelen Plateau by the Earth's rotation. The Kerguelen DWBC was likely responsible for transport between Prydz Bay and the Kerguelen Plateau during the Eocene (Scher et al., 2014) and would have allowed transportation of Southern Ocean-derived bottom waters and Antarctic-sourced terrigenous sediment around our study sites. Neodymium signatures representing proto-CDW have also been reconstructed for the late Eocene using fossil fish teeth from the Southern Kerguelen Plateau (ODP Site 738) (Scher et al., 2014). Proto-AABW is thought to have existed by the early Eocene, based on the distribution of hiatuses in the Indian Ocean (Ramsay et al., 1994) and unradiogenic Nd compositions reconstructed at Kerguelen Plateau and the Indian Ocean basin ($\varepsilon_{Nd} = -9.3 \pm 1.5$; Huck et al., 2017).

2.3. Age Model

The original magnetic reversal stratigraphy for the upper Eocene to lower Oligocene sections of ODP Sites 744 and 748 (Inokuchi & Heider, 1992; Keating & Sakai, 1991) was updated with u-channel samples (Roberts et al., 2003). New magnetic reversal datums were used to constrain diatom datums of Baldauf and Barron (1991) and Harwood et al. (1992). Recently, the integrated magnetobiostratigraphic framework for these sites has been refined using stable isotope chemostratigraphy (Bohaty et al., 2014). Maxima and minima in $\delta^{18}O$ and $\delta^{13}C$ of the fine fraction throughout the Southern Ocean have been shown to be synchronous within the uncertainty of the magnetobiostratigraphy and are used to enhance correlations between sites (Bohaty et al., 2014). All ages are reported relative to the 2012 Geologic Time Scale (Gradstein et al., 2012).

3. Analytical Methods

3.1. Fossil Fish Teeth

Forty-seven samples were taken from ODP Hole 744A (samples between 101.84 and 152.64 m below seafloor) and 151 samples from ODP Hole 748B (samples between 65.67 and 125.97 m below seafloor). Fossil fish teeth were handpicked from the >125 μm fraction of 204 washed sediment samples. Fish teeth were treated with reductive, oxidative, and partial dissolution steps (Boyle, 1981; Boyle & Keigwin, 1985) to chemically remove ferromanganese coatings. Treated samples were transferred to acid-cleaned microcentrifuge tubes and dissolved in 50 μL of 0.25 M HCl. Samples were processed for ion and cation exchange chemistry using the method of Scher and Delaney (2010). Briefly, dissolved fish teeth were loaded on to LnSpec resin

(50–100 μm), using microcolumns made from heat shrink Teflon tubing, and the Nd was collected using 0.25 M HCl.

3.2. Neodymium Isotopic Analysis

The measurement of Nd isotopes was carried out using a Neptune multicollector-inductively coupled plasma mass spectrometer (MC-ICPMS) at the University of South Carolina, run in static mode, using an Apex inlet system (ESI; Ohama, NE) and an X skimmer cone. The Nd isotope analysis consisted of 40 cycles of 8 s integration time for all masses of Nd and masses of 147 and 149, where mass 147 was used to monitor and correct for the isobaric interference of ^{144}Sm on mass 144.

The JNdi-1 isotope standard was run every fifth sample, and the average value for the analytical session was used to normalize the measured Nd isotope ratios to JNdi-1 = 0.512115. The instrumental uncertainty over the time period of analysis was 0.000011 (2σ, n = 129). Fossil fish tooth ^{143}Nd/^{144}Nd data were corrected for the radiogenic ingrowth of ^{143}Nd since the time of deposition, based on a ^{147}Sm/^{144}Nd ratio of 0.133 from samples of a similar age at Kerguelen Plateau Site 738 (Scher et al., 2011) (see supporting information Figure S1).

3.3. Paleolatitude and Paleodepth of Sites

We derive paleodepths for our study sites and comparison sites (Table 1) based on the present-day isostatically unloaded basement depth, LIP emplacement age, and an age-depth subsidence model for oceanic crust based on Stein and Stein (1992). We isostatically load sediment through time based on the observed sediment age-depth models for each site and apply the isostatic correction outlined in Sykes (1996) (see supporting information). We derive paleodepths of ~1,200 m (Site 748, Hole 748B) and ~2,250 m (Site 744, Hole 744A), which are deeper than previously published depths (Site 748, Hole 748B: ~900 m (Bohaty et al., 2009); Site 744, Hole 744A: ~1,900 (Bohaty et al., 2012)). This difference results from our choice of oceanic subsidence model (i.e., Stein & Stein, 1992), which has shown to better predict oceanic basement depth and thermally rejuvenated lithosphere through time (Müller et al., 2008) compared to subsidence models which only reflect changes related to aging of oceanic plates (e.g., Parsons & Sclater, 1977) (which is used within the approaches of Coffin, 1992 and Bohaty et al., 2009).

The paleolatitudes of our study sites (Sites 744 and 748) vary by 2–3° to their present-day latitudes. During the time period of interest (36–23 Ma), paleolatitudes for our study sites are ~58–63°S (Site 744) and ~55–60°S (Site 748), based on the ranges derived from plate reconstructions (e.g., Müller et al., 2016; Seton et al., 2012), and those available from van Hinsbergen et al. (2015) (Table 1). The paleolatitudes derived for other ODP sites referred to in this study are between 32°S and 66°S (Figure 2) and range by up to 8° between plate reconstructions (Table 1).

4. Results

The ε_{Nd} records from the two sites in this study are remarkably similar. Both sites show a small but significant long-term ε_{Nd} decrease of around 1 ε_{Nd} and illustrate several short-term fluctuations that are synchronous at the resolution of this study. In general, the more Antarctic proximal location (Site 744) has less radiogenic ε_{Nd} signatures with short-term excursions that reach lower ε_{Nd} values.

The Nd isotopic composition of fish tooth samples generated from Site 744 have $\varepsilon_{Nd}(t)$ values between −7.2 ± 0.3 (at 34.4 Ma) and −9.3 ± 0.4 (at 33.7 Ma) (Figure 3a), with a mean value of $\varepsilon_{Nd}(t)$ = −7.9. The Nd isotopic composition of fish tooth samples from Site 748 is more radiogenic than those at Site 744, with $\varepsilon_{Nd}(t)$ values between −6.5 ± 0.1 (at 34.5 Ma) and −8.3 ± 0.5 (at 32.5 Ma) (Figure 3a), with a mean value of $\varepsilon_{Nd}(t)$ = −7.3. Both Site 744 and Site 748 show an Nd isotope excursion over the EOT interval (when inferred across the hiatus in the cores): Site 744 shows a large negative excursion (from $\varepsilon_{Nd}(t)$ values around −7.5 to −9.3 ± 0.4 at 33.7 Ma) (Figure 3b), while Site 748 displays a smaller Nd isotope excursion (from $\varepsilon_{Nd}(t)$ values around −7 to −8.3 ± 0.1 at 33.7 Ma) (Figure 3b). The long-term decrease in the Nd isotopic composition is subtle due to the short-term excursions toward less radiogenic values. Before and after the EOT excursion the ε_{Nd} value at Site 744 is around −7.25 and at Site 748 is around −7. At the end of the record ε_{Nd} values for both sites are around −8 to −8.25.

Table 1
Comparison of Present-Day and Oligocene (~30 Ma) Depths and Latitudes

			Present-day		Oligocene (~30 Ma)				
						Paleolatitude (°S)			
Site	Hole	Region	Depth (m)	Latitude (°S)	Paleodepth (m)	T2012	BC2002	Seton et al. (2012)	Müller et al. (2016)
748	B	S Kerguelen Plateau	1,287.5	58.441	1,200	55.44	57.72	57.0578	60.3882
744	A	S Kerguelen Plateau	2,307.3	61.579	2,250	58.29	60.51	60.1737	63.5598
738	B	S Kerguelen Plateau	2,252.7	62.709	2,100	59.37	61.55	61.2762	64.737
689	B	Maud Rise	2,080	64.517	1,900	67.58	69.07	64.9213	63.6731
1090	B	Agulhas Ridge	3,698.6	42.9137	3,400	49.93	51.11	47.1674	46.0179
1263	A	Walvis Ridge	2,717.1	28.5328	2,400	35.63	36.65	32.6517	31.2332
1264	A	Walvis Ridge	2,507	28.5325	2,350	35.63	36.65	32.6525	31.2394
1172	A	East Tasman Plateau	2,621.9	43.9598	2,400	54.85	53.67	58.4039	61.1877
1124	C	Hikurangi Plateau	3,967.5	39.4984	3,850	44.36	42.49	46.3610	45.7359
757	B	Ninetyeast Ridge	1,652.1	17.0243	1,150	27.61	29.35	29.3955	32.7201

Note. T2012 (Torsvik et al., 2012) and BC2002 (Besse & Courtillot, 2002) are based on the reference frame from van Hinsbergen et al. (2015).

Unconformities in both sections result in a hiatus within the EOT interval (34.2–33.7 Ma). Neodymium isotope values at both sites decrease prior to the hiatus and increase following the hiatus. At Site 748, $\varepsilon_{Nd}(t)$ values decrease by 1 ε_{Nd} unit (from −6.6 to −7.5) in the 400 kyr preceding the onset of the hiatus across the Eocene-Oligocene boundary. The record from Site 744 is lower resolution; however, a 0.5 ε_{Nd} decrease

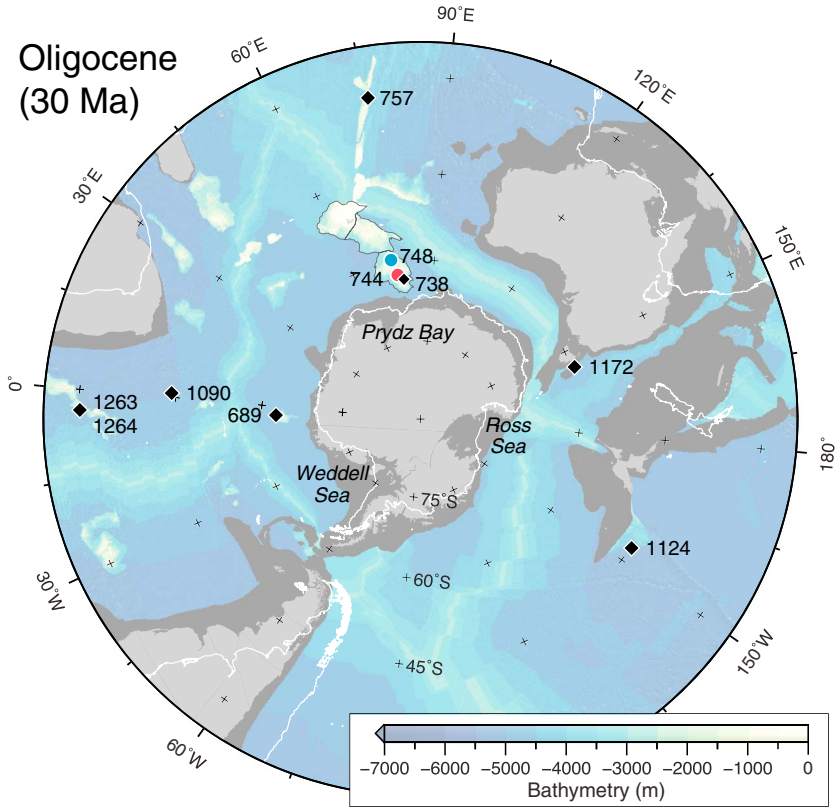

Figure 2. Plate tectonic reconstruction for 30 Ma (Oligocene) showing the location of the study sites and other sites referred to in this study. Reconstruction is based on Müller et al. (2016). Paleobathymetry is derived using the method outlined in Müller et al. (2008) and is illuminated by reconstructed marine gravity anomalies from Sandwell et al. (2014) to illustrate regions of presently preserved oceanic crust. Present-day coastlines (white line), the reconstructed coastlines based on their present-day outline (solid light gray), regions of nonoceanic crust (e.g., continental shelves) (dark gray), and the paleoposition of the Kerguelen Plateau (gray outline) are shown.

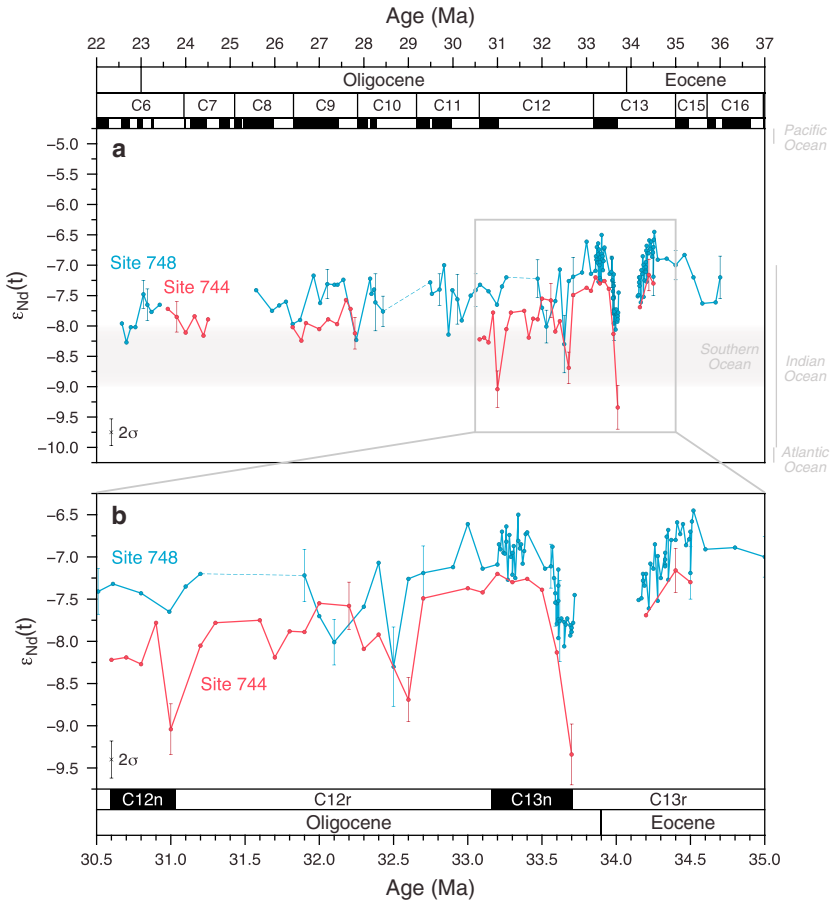

Figure 3. Fossil fish teeth $\varepsilon_{Nd}(t)$ records generated in this study from ODP Sites 744 and 748, with uncertainties larger than instrumental uncertainty for the time period of analysis shown (0.000011, 2σ, $n = 129$). Sampling gaps are shown as dashed lines. Present-day ε_{Nd} endmember ranges (gray) for the Pacific, Indian, and Atlantic are from Goldstein and Hemming (2003). (a) Full fish tooth Nd record generated for this study. (b) Fish tooth Nd record from this study across the EOT only.

precedes the hiatus. The $\varepsilon_{Nd}(t)$ values at both sites recover to pre-EOT values around 33.5 Ma, though the magnitude of the recovery of $\varepsilon_{Nd}(t)$ values at Site 744 is twice as large compared to Site 748.

5. Discussion

During the Eocene, the Kerguelen Plateau was likely influenced by a water mass that carried circumpolar waters (i.e., proto-CDW) (Scher et al., 2014). The Nd isotope records from fossil fish teeth generated in this study reveal a long-term decrease in $\varepsilon_{Nd}(t)$, from -6.5 to -7.5 in the late Eocene to -7.5 to -8.3 $\varepsilon_{Nd}(t)$ by the late Oligocene, which resembles estimated late Eocene CDW values ($\varepsilon_{Nd}(t) = -7.5$ to -8.0; Scher et al., 2014). The similarity in $\varepsilon_{Nd}(t)$ trends to more negative values at the Southern Kerguelen Plateau and Maud Rise suggests that both locations were likely influenced by a common water mass, such as proto-CDW (Figure 4). We interpret the water mass around Sites 744 and 748 to include a significant proto-CDW component during our study period, based on the integration of our Nd isotope records with the interpreted location of proto-PF (Cooke et al., 2002) and water mass from Nd isotope records from other Southern Ocean sites (Scher et al., 2014).

Reconstructions of the position of the proto-PF around the Kerguelen Plateau during the Eocene and Oligocene suggest that the proto-PF likely passed south of Site 748 and migrated northward since the Eocene, based on the presence of bolboforms (Cooke et al., 2002). The northward migration of the proto-PF is also supported by the significant cooling of surface and intermediate waters around Kerguelen Plateau during the late Eocene and early Oligocene, based on benthic foraminiferal $\delta^{18}O$ values at Site 744 (Salamy & Zachos, 1999) and Site 748 (Zachos, Berggren, et al., 1992). Given that the modern-day topography

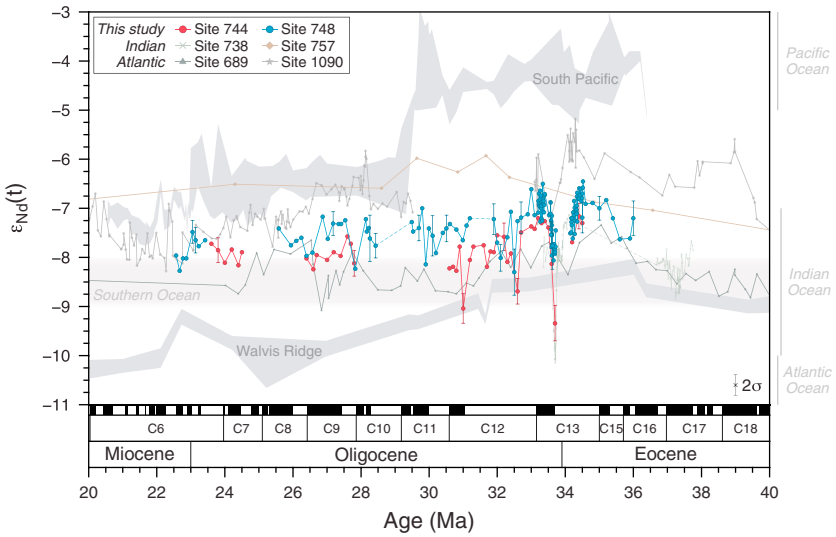

Figure 4. Comparison of fossil fish teeth $\varepsilon_{Nd}(t)$ records generated in this study (southern Kerguelen Plateau) and fossil fish teeth derived Nd records from Southern Ocean sites in the Pacific, Atlantic, and Indian Ocean sectors, including Site 738 (Scher et al., 2011), Site 757 (Martin & Scher, 2006), Site 689 (Scher & Martin, 2004), and Site 1090 (Scher & Martin, 2006, 2008). The Pacific sector ("South Pacific") of the Southern Ocean endmember is based on Sites 1124 and 1172 (Scher et al., 2015), while the Walvis ridge endmember is based on Sites 1263 and 1264 (Via & Thomas, 2006). All records have been converted into the timescale of Gradstein et al. (2012). Gray shaded regions and ranges refer to present-day ε_{Nd} endmember values (Goldstein & Hemming, 2003).

of the Kerguelen Plateau influences the pathway of the Southern Ocean fronts (Sokolov & Rintoul, 2009), it is possible that the Kerguelen Plateau may have similarly deviated the pathway of the proto-PF during the Eocene and Oligocene. The paleobathymetry of the southern and central Kerguelen Plateau was sufficiently deep and unlikely to have formed a barrier on water transport pathways during the Eocene; however, the inferred subaerial emplacement of Skiff Bank (~68 Ma; Duncan, 2002) and shallow paleodepth estimates (870 m; Wallace, 2002) associated with northern Kerguelen Plateau emplacement at ~40 Ma (Duncan, 2002) likely influenced the pathways of Southern Ocean protofronts. We infer that the proto-PF passed north of Site 748 before our record begins, as we do not see any significant evidence for changes in water mass mixing between the late Eocene and late Oligocene, and cooling of waters around the southern Kerguelen Plateau could occur without a change in water mass mixing as a result of the globally cooling climate.

5.1. Long-Term Decrease in $\varepsilon_{Nd}(t)$

We observe a long-term decrease in our fossil fish teeth Nd record from Sites 744 and Sites 748 from $\varepsilon_{Nd}(t)$ values from −6.5 to −7.5 in the late Eocene to −7.5 to −8.3 by the late Oligocene (Figure 3). Decreasing fossil fish tooth $\varepsilon_{Nd}(t)$ values during the Oligocene have been observed at other sites in the Atlantic sector of the Southern Ocean, that is, Agulhas Ridge (Site 1090; Scher & Martin, 2008) and the Walvis Ridge (Sites 1262, 1263, and 1264) (Via & Thomas, 2006) (Figure 4) and are suggested to be due to an increase in NCW export from ~33 Ma (Via & Thomas, 2006). An increase in the flux of NCW into the Southern Ocean would cause a decrease in $\varepsilon_{Nd}(t)$ values into the Oligocene, due to the mixing of unradiogenic NCW (ε_{Nd} = −10.07 ± 0.10; ferromanganese crust sample ALV-539; O'nions et al., 1998) with proto-CDW (i.e., $\varepsilon_{Nd}(t)$ = −7.5 to −8 in the late Eocene; Scher et al., 2014). Comparison of benthic foraminiferal $\delta^{18}O$ records suggests the inception of NCW formation around the middle to late Eocene (~38.5 Ma) in the Labrador Sea (Borrelli et al., 2014), strengthening around 35 Ma (Langton et al., 2016). The presence of NCW in the deep Atlantic by the earliest Oligocene is also supported by the onset of drift deposition in the northeast Atlantic (Davies et al., 2001) and $\delta^{13}C$ deep-water aging gradients (Elsworth et al., 2017), though Abelson and Erez (2017) suggest NCW and the onset of modern-like Atlantic meridional overturning circulation (AMOC) occurred during the late Eocene, immediately before the EOT. We interpret the long-term decreasing trend at our study sites to be related to the increase in NCW contribution to proto-CDW. We note that it is also feasible that the decrease in our ε_{Nd} values could be due to a change in the value of NCW itself, rather than a change in its flux; however, there is currently no evidence to support this scenario. The similar long-term decrease in the Nd isotope

records from both Sites 744 and 748 additionally support the influence of a common water mass around Kerguelen Plateau, for example, proto-CDW. We suggest that the long-term decrease in proto-CDW ε_{Nd} values is not related to an increased contribution from proto-AABW. However, we suggest that the entrainment and mixing of proto-AABW into proto-CDW resulted in the offset in ε_{Nd} values between our study sites during the late Eocene and Oligocene (section 5.2).

An alternative mechanism for the decreasing $\varepsilon_{Nd}(t)$ values in proto-CDW waters during the Oligocene is an increasing contribution from Southern Ocean-sourced bottom waters. Bottom water formation (e.g., a proto-AABW) in the Southern Ocean has been proposed since the early Eocene, in modern day locations such as the Weddell Sea (Thomas et al., 2003), the Ross Sea (Douglas et al., 2014; Hollis et al., 2012; Thomas et al., 2014), or near Adélie Land (Huck et al., 2017). Proto-AABW forming during the Eocene and Oligocene is likely to have similar ε_{Nd} values to modern day, due to the geological similarity in the contributing source regions on Antarctica in present-day locations of bottom water formation. Therefore, while it is possible that the long-term decrease in our ε_{Nd} values at Sites 744 and 748 may reflect a change in the contribution of proto-AABW, recent insights into the onset of NCW export after the EOT imply the long-term change in our record is related to the increase of NCW, rather than a change in proto-AABW.

5.2. Offset Between Neodymium Records From Sites 744 and 748

The $\varepsilon_{Nd}(t)$ record derived from Site 744 is less radiogenic than Site 748 for the duration of our study period. This offset could be attributed to a greater contribution of proto-AABW influencing Site 744, possibly due to its closer proximity to Antarctica and deeper paleodepth (~2,250 m) compared to Site 748. Proto-AABW formation in the Weddell Sea (Thomas et al., 2003) or the Ross Sea (Douglas et al., 2014; Hollis et al., 2012; Thomas et al., 2014) may have influenced our sites. The major circulation pathways from the Weddell Sea bottom water source is thought to flow north of southern Kerguelen Plateau rather than through the Princess Elizabeth Trough and past our southern Kerguelen Plateau sites during the early Eocene (Thomas et al., 2003); however, this pathway is somewhat speculative. Similarly, unradiogenic waters may have been sourced from Adélie Coast-Wilkes Land bottom waters flowing from the Australian-Antarctic Basin, westward toward the Kerguelen Plateau ($\varepsilon_{Nd} = -10.6$; Huck et al., 2017). The Prydz Bay gyre would additionally have allowed for redistribution of proto-AABW and associated entrained dissolved Nd from short-lived weathering activity in the Prydz Bay region to the Kerguelen Plateau.

During the Eocene and Oligocene, sinking of the dense waters associated with proto-AABW and mixing with lower CDW would more greatly influence Site 744. Our new records provide observational support for increasing proto-AABW influence with closer proximity to Antarctica and increasing depth. The Nd isotope record from Site 744, which is ~1,000 m deeper and closer to the Antarctic continent than Site 748, is consistently ~0.5 ε_{Nd} less radiogenic than the record from Site 748 (Figures 3 and 5). We suggest that while both Sites 744 and 748 were influenced by proto-CDW, based on their similar long-term trend, a greater contribution of proto-AABW to the deeper Site 744 is also preserved resulting in the observed ~0.5 ε_{Nd} offset.

5.2.1. Evidence of Glacial Weathering Events in Site 744

The history of Antarctic ice sheet stability during the Oligocene is still very much a matter of debate. High frequency variability in the fish tooth ε_{Nd} records from Antarctic-proximal marine sediments has been interpreted as detecting changes in the contribution of dissolved Nd during erosional events resulting from late Eocene and EOT glacial pulses on Antarctica (Scher et al., 2011, 2014). Surges of weathering associated with ice growth at the EOT are manifested as negative ε_{Nd} excursions on southern Kerguelen Plateau (Scher et al., 2011), and can also be observed in Site 744 in the early Oligocene (Figure 3). While the short excursions in the fish tooth Nd isotope record are somewhat poorly resolved, we suggest these isotope excursions at Site 744 represent a local/regional response in seawater chemistry to Antarctic glacial weathering pulses as an increase in the contribution of dissolved unradiogenic Nd from the nearby Lambert Graben to the surrounding seawater in Prydz Bay would result in less radiogenic ε_{Nd} values preserved in the fish teeth at Site 744.

Prydz Bay, via the Lambert Graben, is believed to be a site of major East Antarctic glacial discharge (DeConto & Pollard, 2003; Strand et al., 2003) during the Oligocene, and a major fluvial output during the late Eocene (Jamieson et al., 2005). Prydz Bay is composed of Precambrian basement with Archean, Proterozoic, and Cambrian terranes and intrusives (Fitzsimons, 2003). The Lambert Graben, which intersects Prydz Bay and

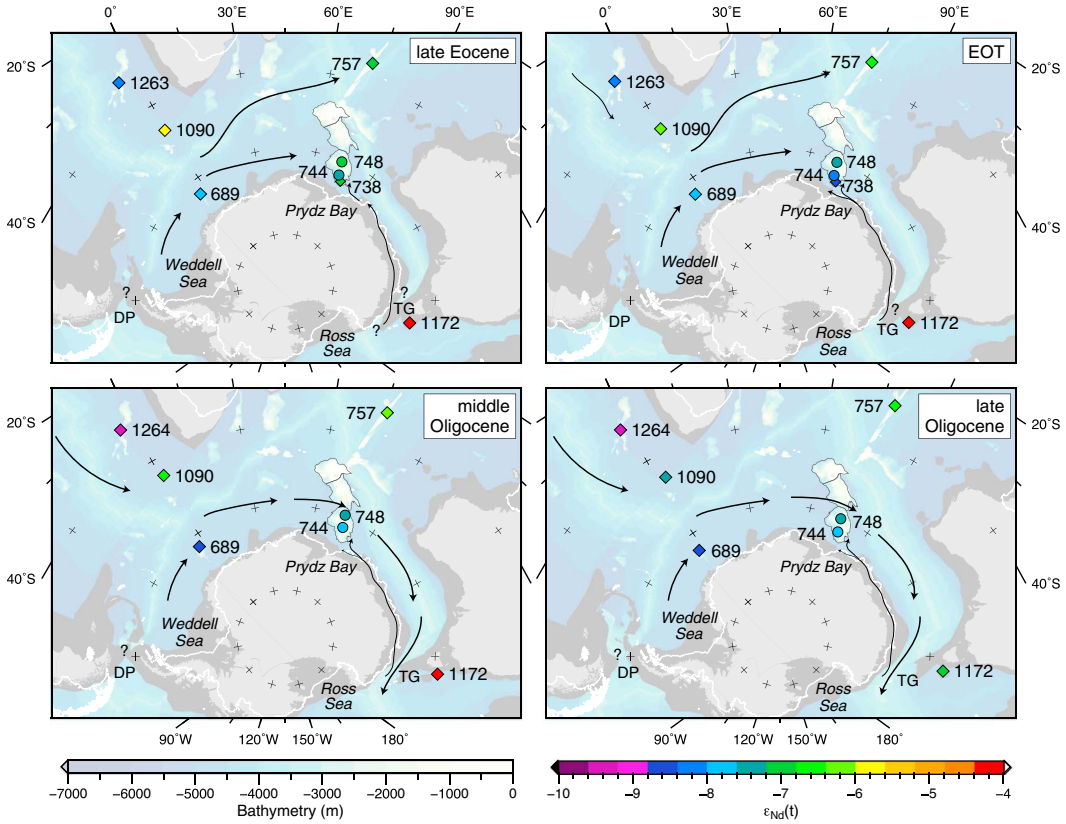

Figure 5. Schematic of water transport pathways from the late Eocene (~36–34 Ma), EOT (33.9–33.5 Ma), middle Oligocene (31–27 Ma), and late Oligocene (25–23 Ma), based on Nd isotope data only. ODP sites are colored based on their average $\varepsilon_{Nd}(t)$ value for each period considered (see supporting information). Plate tectonic reconstructions are based on Müller et al. (2016), with paleobathymetry derived using the method outlined in Müller et al. (2008). Present-day coastlines (white line), the reconstructed position of the present-day coastlines (solid light gray), and regions of nonoceanic crust (e.g., continental shelves) (dark gray) are also shown. The paleoposition of the Kerguelen Plateau is shown as a gray outline.

extends 700 km inland, represents a failed arm of a Mesozoic triple junction associated with Gondwana breakup (Stagg, 1985). At present day, the Lambert Glacier-Amery Ice Shelf system discharges around 16% of the grounded East Antarctic Ice Sheet into Prydz Bay (Fricker et al., 2000; O'Brien et al., 2007). Sediments from Prydz Bay have ε_{Nd} values ranging between −17.7 and −21.3 (Roy et al., 2007), providing a suitable source of unradiogenic material to our study sites. While this is not the only possible source of unradiogenic material to our study sites, Prydz Bay is the main trunk in the preglacial river network (Wilson & Luyendyk, 2009) and is therefore the most likely source of unradiogenic material.

Both study sites preserve the onset and recovery of the negative ε_{Nd} excursion associated with major expansion of ice sheets and enhanced erosion of bedrock on Antarctica across the EOT (Scher et al., 2011). However, Site 744 ε_{Nd} values appear to have been more strongly influenced by changes in Antarctic weathering across the EOT, for example, Site 744 has a negative excursion to −9.3 ± 0.4 $\varepsilon_{Nd}(t)$ at 33.7 Ma and recovers to around −7.3 after 33.5 Ma, while Site 748 has a negative excursion to −8.1 ± 0.1 $\varepsilon_{Nd}(t)$ at 33.65 Ma and recovers to −7 after 33.5 Ma (Figure 3). This is likely due to the proximity of Site 744 to Prydz Bay and its greater influence of proto-AABW, which transports the erosional signal to Site 744. In particular, Nd isotope ratios from Site 744 show a significant drop by 1.2 ± 0.3 ε_{Nd} at 32.6 Ma. This may be a response to widespread expansion of the Antarctic ice sheet, already observed by Galeotti et al. (2016) as an increase in coarse grains at 32.8 Ma in marine sediments from the Ross Sea.

5.3. Other Potential Terrigenous Sources of Neodymium

During the Eocene and Oligocene, the southern Kerguelen Plateau was remote relative to all sources of terrigenous material except for the adjacent Prydz Bay. Other possible sources of Nd include nearby

hydrothermal activity and/or volcanogenic sediments associated with the emplacement of northern Kerguelen Plateau, and the weathering of glaciers and IRD from East Antarctica, for example, at ~33.7 Ma (Scher et al., 2011; Zachos, Breza, et al., 1992).

The timing of northern Kerguelen Plateau emplacement (40–34 Ma; Duncan, 2002) overlaps with our fish tooth Nd isotope record (36–23 Ma) from the southern Kerguelen Plateau, which raises the possibility of contributions from volcanogenic sediments and/or hydrothermal products with radiogenic Nd isotope signatures. Basaltic samples dredged between the Kerguelen Archipelago and Heard Island exhibit radiogenic Nd isotope compositions, with ε_{Nd} values from −1.95 to 6.26 (Weis et al., 2002). Thus, the influence of volcanic input associated with the eruption of northern Kerguelen Plateau would result in an increase in our fish tooth Nd record to more positive ε_{Nd} values; however, this trend is not observed in our record. Additionally, the predominant northward flow of the modern Kerguelen DWBC (Fukamachi et al., 2010) and its inferred northward flow in the Eocene (Scher et al., 2014) suggests that volcanogenic contributions transported to our study sites by deep currents from the eruption of the northern Kerguelen Plateau would be unlikely. The occurrence of IRD at ~33.7 Ma (when converted into the Gradstein et al., 2012 timescale) has also been established at Sites 748 (Zachos, Breza, et al., 1992) and 738 (Scher et al., 2011) and represents short episodes of ice rafting carrying terrigenous material derived from a metamorphic and/or plutonic terrane, such as those found on the Antarctic continent (Pierce et al., 2014). However, previous work has found that fossil fish teeth are not affected by postburial uptake of rare earth elements from IRD (Scher et al., 2011). Finally, hydrothermal activity has been shown to have a negligible effect on oceanic Nd isotope ratios (Halliday et al., 1992); however, this study is based on hydrothermal activity at a ridge axis rather than the emplacement of a large igneous body. Based on the radiogenic Nd isotope ratios (ε_{Nd} = −1.95 to 6.326) of the northern Kerguelen Plateau, compared to our unradiogenic fish teeth Nd record (ε_{Nd} = −7 to −8), we suggest that the northern Kerguelen Plateau emplacement is not a source of Nd to our study sites.

5.4. Implications for the Drake Passage

The timing of the tectonic opening and deepening of the Tasman Gateway (e.g., ~33 Ma; Stickley et al., 2004), along with a number of interpretations for the Drake Passage (e.g., shallow/intermediate opening from 50 Ma, deep water gateway opening from ~30–34 Ma; Eagles & Jokat, 2014; Livermore et al., 2005, 2007), coincides with our study period (36–23 Ma). The opening of the Tasman Gateway was a distal event far downstream of the circum-Antarctic relative to our study sites. Although the westward flowing ASC may have possibly transported Pacific waters toward Kerguelen Plateau (Scher et al., 2015), they were probably not detectable due the similarity in ε_{Nd} values to our record (~ − 7.5 ε_{Nd}) from the Kerguelen Plateau. However, since our study sites are eastward of the Scotia Sea, and downstream of the oceanic gateway, we expect to capture large changes water mass communication related to the opening of the Drake Passage.

A significant opening of the Drake Passage during the late Eocene/Oligocene should result in a shift in ε_{Nd} values on Kerguelen Plateau toward more radiogenic compositions, reflecting an increased input of Pacific waters to proto-CDW. However, the long term ε_{Nd} trend is opposite from this prediction. Our study sites reveal a decrease in ε_{Nd} values over the study interval, implying that no change in Pacific throughflow was initiated by mixing through the Drake Passage during the Oligocene. Since our $\varepsilon_{Nd}(t)$ values (between −7.5 and −8 at Site 748) during the Oligocene are comparable to modern CDW (ε_{Nd} = −8.5; Stichel et al., 2012), we infer that Oligocene water mass composition was similar to present day. Consequently, we propose that the inception of water mass mixing through the Drake Passage preceded the timing of our fossil fish tooth record (36–23 Ma), which is consistent with the published timing of initial water mixing through the Drake Passage suggested based on existing proxy evidence (41–37 Ma; Diester-Haass & Zahn, 1996; Scher & Martin, 2006). This timing is also consistent with plate tectonic reconstructions supporting an early opening of Drake Passage (e.g., Eagles & Jokat, 2014; Livermore et al., 2005, 2007) and suggests that remnant volcanic arcs in the Scotia Sea may not have formed a barrier to Southern Ocean circulation until the Miocene (~12 Ma), as has been proposed (Dalziel et al., 2013).

6. Summary and Conclusion

New Nd isotope records from the southern Kerguelen Plateau preserve a proto-CDW signal during the late Eocene to late Oligocene. Site 748 preserves a gradual shift to less radiogenic Nd isotope values, with ε_{Nd}

values around −6.5 to −7.5 in the late Eocene to ε_{Nd} values between −7.5 and −8.3 by the late Oligocene, which we attribute to an increased contribution of NCW. The long-term unradiogenic trend in our fish tooth Nd isotope record supports previous work, which infers an early to middle Eocene timing of mixing between the Pacific and Atlantic basins via the Drake Passage, prior to our study interval. We find a consistent ~0.5 ε_{Nd} offset between Site 744 (less radiogenic) and Site 748 (more radiogenic), which we interpret as an increasing proto-AABW influence associated with the closer proximity of Site 744 to the Antarctic continent. Both study sites show large excursions toward less radiogenic values at the EOT and in the early Oligocene—the magnitude of the response at Site 744 is greater than Site 748, and Site 744 additionally preserves short-frequency variability in the early Oligocene, further supporting a higher proto-AABW contribution at this location and its transport of dissolved Nd produced by enhanced erosion during glacial advance and retreat on Antarctica. The fish tooth Nd record at Site 748 does not preserve this high-frequency variability, indicating a reduced influence of AABW at this location. We suggest that Maud Rise and the southern Kerguelen Plateau were influenced by a common water mass (proto-CDW) by the Oligocene, based on the similar less radiogenic trend preserved by these sites. Future work such as high-resolution sampling and analysis of Site 744 may provide further insight into the early glacial history of East Antarctica.

Acknowledgments
We thank Steven Bohaty for sharing his updated age model for ODP Sites 744 and 748. We also thank the Editor and two anonymous reviewers for their comments, which has improved the quality of this manuscript. N. M. W. was supported by an Australian Postgraduate Award, H. D. S. by NSF OCE 1155630, M. S. by ARC grant FT130101564, and B. D. D. by the Marine Science Program at the University of South Carolina. Figures were constructed using Generic Mapping Tools. The Nd isotope data generated in this study are available in Tables S1 and S2 of the supporting information.

References

Abelson, M., Agnon, A., & Almogi-Labin, A. (2008). Indications for control of the Iceland plume on the Eocene–Oligocene "greenhouse–icehouse" climate transition. *Earth and Planetary Science Letters*, *265*(1-2), 33–48. https://doi.org/10.1016/j.epsl.2007.09.021

Abelson, M., & Erez, J. (2017). The onset of modern-like Atlantic meridional overturning circulation at the Eocene-Oligocene transition: Evidence, causes, and possible implications for global cooling. *Geochemistry, Geophysics, Geosystems*, *18*, 2177–2199. https://doi.org/10.1002/2017GC006826

Allègre, C. J., Louvat, P., Gaillardet, J., Meynadier, L., Rad, S., & Capmas, F. (2010). The fundamental role of island arc weathering in the oceanic Sr isotope budget. *Earth and Planetary Science Letters*, *292*(1-2), 51–56. https://doi.org/10.1016/j.epsl.2010.01.019

Amante, C., & Eakins, B. (2009). ETOPO1 1 arc-minute global relief model: Procedures, data sources and analysis, NOAA Technical Memorandum NESDIS NGDC-24. https://doi.org/10.7289/V5C8276M

Arsouze, T., Dutay, J., Lacan, F., & Jeandel, C. (2009). Reconstructing the Nd oceanic cycle using a coupled dynamical-biogeochemical model. *Biogeosciences*, *6*(12), 2829–2846. https://doi.org/10.5194/bg-6-2829-2009

Baldauf, J. G., & Barron, J. A. (1991). Diatom biostratigraphy: Kerguelen Plateau and Prydz Bay regions Of the Southern Ocean. In J. A. Barron, & B. Larsen (Eds.), *Proceedings of the Ocean Drilling Program, Scientific Results* (Vol. 119, pp. 547–598). College Station, TX: Ocean Drilling Program.

Barker, P., & Burrell, J. (1977). The opening of Drake passage. *Marine Geology*, *25*(1-3), 15–34. https://doi.org/10.1016/0025-3227(77)90045-7

Belkin, I. M., & Gordon, A. L. (1996). Southern Ocean fronts from the Greenwich meridian to Tasmania. *Journal of Geophysical Research*, *101*, 3675–3696. https://doi.org/10.1029/95JC02750

Bénard, F., Callot, J.-P., Vially, R., Schmitz, J., Roest, W., Patriat, M., … Team, T. E. (2010). The Kerguelen plateau: Records from a long-living/composite microcontinent. *Marine and Petroleum Geology*, *27*(3), 633–649. https://doi.org/10.1016/j.marpetgeo.2009.08.011

Besse, J., & Courtillot, V. (2002). Apparent and true polar wander and the geometry of the geomagnetic field over the last 200 Myr. *Journal of Geophysical Research*, *107*(B11), 2300. https://doi.org/10.1029/2000JB000050

Bohaty, S. M., Scher, H. D., Zachos, J. C., Liebrand, D., & Paelike, H. (2014). Episodic cooling and glacial initiation during the Late Eocene 'Pre-Icehouse' interval. Paper presented at the 32th SCAR Biennial Meetings, Auckland, NZ, Aug. 23–Sept. 3, 2014.

Bohaty, S. M., Zachos, J. C., & Delaney, M. L. (2012). Foraminiferal Mg/Ca evidence for Southern Ocean cooling across the Eocene–Oligocene transition. *Earth and Planetary Science Letters*, *317*, 251–261.

Bohaty, S. M., Zachos, J. C., Florindo, F., & Delaney, M. L. (2009). Coupled greenhouse warming and deep-sea acidification in the middle Eocene. *Paleoceanography*, *24*, PA2207. https://doi.org/10.1029/2008PA001676

Borchers, A., Voigt, I., Kuhn, G., & Diekmann, B. (2011). Mineralogy of glaciomarine sediments from the Prydz Bay–Kerguelen region: Relation to modern depositional environments. *Antarctic Science*, *23*(2), 164–179. https://doi.org/10.1017/S0954102010000830

Borrelli, C., Cramer, B. S., & Katz, M. E. (2014). Bipolar Atlantic deepwater circulation in the middle-late Eocene: Effects of Southern Ocean gateway openings. *Paleoceanography*, *29*, 308–327. https://doi.org/10.1002/2012PA002444

Boyle, E. A. (1981). Cadmium, zinc, copper, and barium in foraminifera tests. *Earth and Planetary Science Letters*, *53*(1), 11–35. https://doi.org/10.1016/0012-821X(81)90022-4

Boyle, E., & Keigwin, L. (1985). Comparison of Atlantic and Pacific paleochemical records for the last 215,000 years: Changes in deep ocean circulation and chemical inventories. *Earth and Planetary Science Letters*, *76*(1-2), 135–150. https://doi.org/10.1016/0012-821X(85)90154-2

Coffin, M. F. (1992). Subsidence of the Kerguelen Plateau: The Atlantis concept. In S. W. Wise, Jr., et al. (Eds.), *Proceedings of the Ocean Drilling Program, Scientific Results* (Vol. 120, pp. 945–949). College Station, TX: Texas A&M University. https://doi.org/10.2973/odp.proc.sr.120.202.1992

Coffin, M. F., Pringle, M., Duncan, R., Gladczenko, T., Storey, M., Müller, R., & Gahagan, L. (2002). Kerguelen hotspot magma output since 130 ma. *Journal of Petrology*, *43*(7), 1121–1137. https://doi.org/10.1093/petrology/43.7.1121

Cooke, P. J., Nelson, C. S., Crundwell, M. P., & Spiegler, D. (2002). Bolboforma as monitors of Cenozoic palaeoceanographic changes in the Southern Ocean. *Palaeogeography, Palaeoclimatology, Palaeoecology*, *188*(1-2), 73–100. https://doi.org/10.1016/S0031-0182(02)00531-X

Dalziel, I., Lawver, L., Pearce, J. A., Barker, P., Hastie, A., Barfod, D., … Davis, M. (2013). A potential barrier to deep Antarctic circumpolar flow until the late Miocene? *Geology*, *41*(9), 947–950. https://doi.org/10.1130/G34352.1

Davies, R., Cartwright, J., Pike, J., & Line, C. (2001). Early Oligocene initiation of North Atlantic deep water formation. *Nature*, *410*(6831), 917–920. https://doi.org/10.1038/35073551

DeConto, R. M., & Pollard, D. (2003). Rapid Cenozoic glaciation of Antarctica induced by declining atmospheric CO_2. *Nature*, *421*(6920), 245–249. https://doi.org/10.1038/nature01290

Diester-Haass, L., & Zahn, R. (1996). Eocene-Oligocene transition in the Southern Ocean: History of water mass circulation and biological productivity. *Geology*, *24*(2), 163–166. https://doi.org/10.1130/0091-7613(1996)024%3C0163:EOTITS%3E2.3.CO;2

Diester-Haass, L., & Zahn, R. (2001). Paleoproductivity increase at the Eocene–Oligocene climatic transition: ODP/DSDP Sites 763 and 592. *Palaeogeography, Palaeoclimatology, Palaeoecology*, *172*(1-2), 153–170. https://doi.org/10.1016/S0031-0182(01)00280-2

Donohue, K. A., Hufford, G. E., & McCartney, M. S. (1999). Sources and transport of the deep western boundary current east of the Kerguelen plateau. *Geophysical Research Letters*, *26*, 851–854. https://doi.org/10.1029/1999GL900099

Douglas, P. M., Affek, H. P., Ivany, L. C., Houben, A. J., Sijp, W. P., Sluijs, A., … Pagani, M. (2014). Pronounced zonal heterogeneity in Eocene southern high-latitude sea surface temperatures. *Proceedings of the National Academy of Sciences of the United States of America*, *111*(18), 6582–6587. https://doi.org/10.1073/pnas.1321441111

Duncan, R. A. (2002). A time frame for construction of the Kerguelen plateau and broken ridge. *Journal of Petrology*, *43*(7), 1109–1119. https://doi.org/10.1093/petrology/43.7.1109

Eagles, G., & Jokat, W. (2014). Tectonic reconstructions for paleobathymetry in drake passage. *Tectonophysics*, *611*, 28–50. https://doi.org/10.1016/j.tecto.2013.11.021

Elsworth, G., Galbraith, E., Halverson, G., & Yang, S. (2017). Enhanced weathering and CO_2 drawdown caused by latest Eocene strengthening of the Atlantic meridional overturning circulation. *Nature Geoscience*, *10*(3), 213–216. https://doi.org/10.1038/ngeo2888

Fitzsimons, I. (2003). Proterozoic basement provinces of southern and southwestern Australia, and their correlation with Antarctica. *Geological Society, London, Special Publications*, *206*(1), 93–130. https://doi.org/10.1144/GSL.SP.2003.206.01.07

Frank, M. (2002). Radiogenic Isotopes: Tracers of past ocean circulation and erosional input. *Reviews of Geophysics*, *40*(1), 1001. https://doi.org/10.1029/2000RG000094

Frey, F., Coffin, M., Wallace, P., & Weis, D. (2003). Leg 183 synthesis: Kerguelen Plateau-Broken Ridge—A large igneous province. *Proceeding of the Ocean Drilling Program, Scientific Results*, *183*, 1–48.

Frey, F., Coffin, M., Wallace, P., Weis, D., Zhao, X., Wise, S., … Reusch, D. (2000). Origin and evolution of a submarine large igneous province: The Kerguelen Plateau and Broken Ridge, southern Indian Ocean. *Earth and Planetary Science Letters*, *176*(1), 73–89. https://doi.org/10.1016/S0012-821X(99)00315-5

Fricker, H. A., Warner, R. C., & Allison, I. (2000). Mass balance of the Lambert Glacier–Amery Ice Shelf system, East Antarctica: A comparison of computed balance fluxes and measured fluxes. *Journal of Glaciology*, *46*(155), 561–570. https://doi.org/10.3189/172756500781832765

Fukamachi, Y., Rintoul, S., Church, J., Aoki, S., Sokolov, S., Rosenberg, M., & Wakatsuchi, M. (2010). Strong export of Antarctic Bottom Water east of the Kerguelen plateau. *Nature Geoscience*, *3*(5), 327–331. https://doi.org/10.1038/ngeo842

Galeotti, S., DeConto, R., Naish, T., Stocchi, P., Florindo, F., Pagani, M., … Pollard, D. (2016). Antarctic ice sheet variability across the Eocene-Oligocene boundary climate transition. *Science*, *352*(6281), 76–80. https://doi.org/10.1126/science.aab0669

Goldstein, S. L., & Hemming, S. R. (2003). Long-lived isotopic tracers in oceanography, paleoceanography, and ice-sheet dynamics. *Treatise on Geochemistry*, *6*, 453–489.

Gradstein, F. M., Ogg, J. G., Schmitz, M., & Ogg, G. (2012). *The geologic time scale 2012*. Boston: Elsevier. https://doi.org/10.1016/B978-0-444-59425-9.00004-4

Halliday, A. N., Davidson, J. P., Holden, P., Owen, R. M., & Olivarez, A. M. (1992). Metalliferous sediments and the scavenging residence time of Nd near hydrothermal vents. *Geophysical Research Letters*, *19*, 761–764. https://doi.org/10.1029/92GL00393

Harwood, D., Lazarus, D., Abelmann, A., Aubry, M., Berggren, W., Heider, F., … Wei, W. (1992). Neogene integrated magnetobiostratigraphy of the central Kerguelen Plateau, Leg 120. Paper presented at Proceedings of the ODP, Sci Results.

Heywood, K. J., Sparrow, M. D., Brown, J., & Dickson, R. R. (1999). Frontal structure and Antarctic bottom water flow through the Princess Elizabeth trough, Antarctica. *Deep Sea Research Part I: Oceanographic Research Papers*, *46*(7), 1181–1200. https://doi.org/10.1016/S0967-0637(98)00108-3

Hollis, C. J., Taylor, K. W., Handley, L., Pancost, R. D., Huber, M., Creech, J. B., … Crampton, J. S. (2012). Early Paleogene temperature history of the Southwest Pacific Ocean: Reconciling proxies and models. *Earth and Planetary Science Letters*, *349*, 53–66.

Huber, M., Brinkhuis, H., Stickley, C. E., Döös, K., Sluijs, A., Warnaar, J., … Williams, G. L. (2004). Eocene circulation of the Southern Ocean: Was Antarctica kept warm by subtropical waters? *Paleoceanography*, *19*, PA4026. https://doi.org/10.1029/2004PA001014

Huck, C. E., van de Flierdt, T., Bohaty, S. M., & Hammond, S. J. (2017). Antarctic climate, Southern Ocean circulation patterns and deep-water formation during the Eocene. *Paleoceanography*, *32*, 674–691. https://doi.org/10.1002/2017PA003135

Inokuchi, H., & Heider, F. (1992). Paleolatitude of the southern Kerguelen Plateau inferred from the Paleomagnetic study of upper Cretaceous basalts. Paper presented at Proceedings of the ODP, Scientific Results.

Jacobsen, S. B., & Wasserburg, G. (1980). Sm-Nd isotopic evolution of chondrites. *Earth and Planetary Science Letters*, *50*(1), 139–155. https://doi.org/10.1016/0012-821X(80)90125-9

Jamieson, S., Hulton, N., Sugden, D., Payne, A., & Taylor, J. (2005). Cenozoic landscape evolution of the Lambert basin, East Antarctica: The relative role of rivers and ice sheets. *Global and Planetary Change*, *45*(1-3), 35–49. https://doi.org/10.1016/j.gloplacha.2004.09.015

Jeandel, C., Arsouze, T., Lacan, F., Techine, P., & Dutay, J.-C. (2007). Isotopic Nd compositions and concentrations of the lithogenic inputs into the ocean: A compilation, with an emphasis on the margins. *Chemical Geology*, *239*(1-2), 156–164. https://doi.org/10.1016/j.chemgeo.2006.11.013

Keating, B. H., & Sakai, H. (1991). Magnetostratigraphic studies of sediments from Site 744, southern Kerguelen Plateau. In J. Barron, et al. (Eds.), *Proceedings of the Ocean Drilling Program*, *Scientific Results*, (Vol. 119, pp. 771–794). College Station, TX: Texas A&M University. https://doi.org/10.2973/odp.proc.sr.119.147.1991

Kennett, J. P. (1977). Cenozoic evolution of Antarctic glaciation, the Circum-Antarctic Ocean, and their impact on global paleoceanography. *Journal of Geophysical Research*, *82*, 3843–3860. https://doi.org/10.1029/JC082i027p03843

Lacan, F., & Jeandel, C. (2001). Tracing Papua New Guinea imprint on the central Equatorial Pacific Ocean using neodymium isotopic compositions and Rare Earth Element patterns. *Earth and Planetary Science Letters*, *186*(3-4), 497–512. https://doi.org/10.1016/S0012-821X(01)00263-1

Lacan, F., & Jeandel, C. (2005a). Acquisition of the neodymium isotopic composition of the North Atlantic Deep Water. *Geochemistry, Geophysics, Geosystems*, *6*, Q12008. https://doi.org/10.1029/2005GC000956

Lacan, F., & Jeandel, C. (2005b). Neodymium isotopes as a new tool for quantifying exchange fluxes at the continent–ocean interface. *Earth and Planetary Science Letters*, *232*(3-4), 245–257. https://doi.org/10.1016/j.epsl.2005.01.004

Lambelet, M., van de Flierdt, T., Crocket, K., Rehkämper, M., Kreissig, K., Coles, B., … Steinfeldt, R. (2016). Neodymium isotopic composition and concentration in the western North Atlantic Ocean: Results from the GEOTRACES GA02 section. *Geochimica et Cosmochimica Acta*, *177*, 1–29. https://doi.org/10.1016/j.gca.2015.12.019

Langton, S. J., Rabideaux, N. M., Borrelli, C., & Katz, M. E. (2016). Southeastern Atlantic deep-water evolution during the late-middle Eocene to earliest Oligocene (ocean drilling program site 1263 and Deep Sea drilling project site 366). *Geosphere*, *12*(3), 1032–1047. https://doi.org/10.1130/GES01268.1

Lear, C. H., Elderfield, H., & Wilson, P. (2000). Cenozoic deep-sea temperatures and global ice volumes from Mg/Ca in benthic foraminiferal calcite. *Science*, *287*(5451), 269–272. https://doi.org/10.1126/science.287.5451.269

Liu, Z., Pagani, M., Zinniker, D., DeConto, R., Huber, M., Brinkhuis, H., … Pearson, A. (2009). Global cooling during the Eocene-Oligocene climate transition. *Science*, *323*(5918), 1187–1190. https://doi.org/10.1126/science.1166368

Livermore, R., Hillenbrand, C. D., Meredith, M., & Eagles, G. (2007). Drake Passage and Cenozoic climate: An open and shut case? *Geochemistry, Geophysics, Geosystems*, *8*, Q01005. https://doi.org/10.1029/2005GC001224

Livermore, R., Nankivell, A., Eagles, G., & Morris, P. (2005). Paleogene opening of Drake passage. *Earth and Planetary Science Letters*, *236*(1-2), 459–470. https://doi.org/10.1016/j.epsl.2005.03.027

Martin, E., & Haley, B. (2000). Fossil fish teeth as proxies for seawater Sr and Nd isotopes. *Geochimica et Cosmochimica Acta*, *64*(5), 835–847. https://doi.org/10.1016/S0016-7037(99)00376-2

Martin, E., & Scher, H. (2006). A Nd isotopic study of southern sourced waters and Indonesian Throughflow at intermediate depths in the Cenozoic Indian Ocean. *Geochemistry, Geophysics, Geosystems*, *7*, Q09N02. https://doi.org/10.1029/2006GC001302

McCartney, M. S., & Donohue, K. A. (2007). A deep cyclonic gyre in the Australian–Antarctic Basin. *Progress in Oceanography*, *75*(4), 675–750. https://doi.org/10.1016/j.pocean.2007.02.008

Miller, K. G., Fairbanks, R. G., & Mountain, G. S. (1987). Tertiary oxygen isotope synthesis, sea level history, and continental margin erosion. *Paleoceanography*, *2*, 1–19. https://doi.org/10.1029/PA002i001p00001

Müller, R. D., Sdrolias, M., Gaina, C., Steinberger, B., & Heine, C. (2008). Long-term sea-level fluctuations driven by ocean basin dynamics. *Science*, *319*(5868), 1357–1362. https://doi.org/10.1126/science.1151540

Müller, R. D., Seton, M., Zahirovic, S., Williams, S. E., Matthews, K. J., Wright, N. M., … Hosseinpour, M. (2016). Ocean basin evolution and global-scale plate reorganization events since Pangea breakup. *Annual Review of Earth and Planetary Sciences*, *44*(1), 107–138. https://doi.org/10.1146/annurev-earth-060115-012211

Munday, D. R., Johnson, H. L., & Marshall, D. P. (2015). The role of ocean gateways in the dynamics and sensitivity to wind stress of the early Antarctic circumpolar current. *Paleoceanography*, *30*, 284–302. https://doi.org/10.1002/2014PA002675

Nicolaysen, K., Frey, F. A., Hodges, K., Weis, D., & Giret, A. (2000). $^{40}Ar/^{39}Ar$ geochronology of flood basalts from the Kerguelen Archipelago, southern Indian Ocean: Implications for Cenozoic eruption rates of the Kerguelen plume. *Earth and Planetary Science Letters*, *174*(3-4), 313–328. https://doi.org/10.1016/S0012-821X(99)00271-X

Nunes Vaz, R. A., & Lennon, G. W. (1996). Physical oceanography of the Prydz Bay region of Antarctic waters. *Deep-Sea Research Part I: Oceanographic Research Papers*, *43*(5), 603–641. https://doi.org/10.1016/0967-0637(96)00028-3

O'Brien, P. E., Goodwin, I., Forsberg, C.-F., Cooper, A. K., & Whitehead, J. (2007). Late Neogene ice drainage changes in Prydz Bay, East Antarctica and the interaction of Antarctic ice sheet evolution and climate. *Palaeogeography, Palaeoclimatology, Palaeoecology*, *245*(3-4), 390–410. https://doi.org/10.1016/j.palaeo.2006.09.002

Ohshima, K. I., Fukamachi, Y., Williams, G. D., Nihashi, S., Roquet, F., Kitade, Y., … Wakatsuchi, M. (2013). Antarctic bottom water production by intense sea-ice formation in the Cape Darnley polynya. *Nature Geoscience*, *6*(3), 235–240. https://doi.org/10.1038/ngeo1738

O'nions, R., Frank, M., Von Blanckenburg, F., & Ling, H.-F. (1998). Secular variation of Nd and Pb isotopes in ferromanganese crusts from the Atlantic, Indian and Pacific oceans. *Earth and Planetary Science Letters*, *155*(1-2), 15–28. https://doi.org/10.1016/S0012-821X(97)00207-0

Orsi, A. H., Whitworth, T., & Nowlin, W. D. (1995). On the meridional extent and fronts of the Antarctic circumpolar current. *Deep Sea Research Part I: Oceanographic Research Papers*, *42*(5), 641–673. https://doi.org/10.1016/0967-0637(95)00021-W

Park, Y. H., Charriaud, E., & Fieux, M. (1998). Thermohaline structure of the Antarctic surface water/winter water in the Indian sector of the Southern Ocean. *Journal of Marine Systems*, *17*(1-4), 5–23. https://doi.org/10.1016/S0924-7963(98)00026-8

Park, Y., Gamberoni, L., & Charriaud, E. (1993). Frontal structure, water masses, and circulation in the Crozet Basin. *Journal of Geophysical Research*, *98*, 12,361–12,385. https://doi.org/10.1029/93JC00938

Park, Y. H., Roquet, F., Durand, I., & Fuda, J.-L. (2008). Large-scale circulation over and around the Northern Kerguelen Plateau. *Deep Sea Research Part II: Topical Studies in Oceanography*, *55*(5-7), 566–581. https://doi.org/10.1016/j.dsr2.2007.12.030

Park, Y. H., Vivier, F., Roquet, F., & Kestenare, E. (2009). Direct observations of the ACC transport across the Kerguelen plateau. *Geophysical Research Letters*, *36*, L18603. https://doi.org/10.1029/2009GL039617

Parsons, B., & Sclater, J. G. (1977). An analysis of the variation of ocean floor bathymetry and heat flow with age. *Journal of Geophysical Research*, *82*, 803–827. https://doi.org/10.1029/JB082i005p00803

Piepgras, D. J., & Wasserburg, G. J. (1980). Neodymium isotopic variations in seawater. *Earth and Planetary Science Letters*, *50*(1), 128–138. https://doi.org/10.1016/0012-821X(80)90124-7

Pierce, E., Hemming, S., Williams, T., van de Flierdt, T., Thomson, S., Reiners, P. W., … Goldstein, S. (2014). A comparison of detrital U–Pb zircon, $^{40}Ar/^{39}Ar$ hornblende, $^{40}Ar/^{39}Ar$ biotite ages in marine sediments off East Antarctica: Implications for the geology of subglacial terrains and provenance studies. *Earth-Science Reviews*, *138*, 156–178. https://doi.org/10.1016/j.earscirev.2014.08.010

Ramsay, A. T., Sykes, T. J., & Kidd, R. B. (1994). Waxing (and waning) lyrical on hiatuses: Eocene-quaternary Indian Ocean hiatuses as proxy indicators of water mass production. *Paleoceanography*, *9*, 857–877. https://doi.org/10.1029/94PA01397

Rempfer, J., Stocker, T. F., Joos, F., Dutay, J.-C., & Siddall, M. (2011). Modelling Nd-isotopes with a coarse resolution ocean circulation model: Sensitivities to model parameters and source/sink distributions. *Geochimica et Cosmochimica Acta*, *75*(20), 5927–5950. https://doi.org/10.1016/j.gca.2011.07.044

Rickli, J., Gutjahr, M., Vance, D., Fischer-Gödde, M., Hillenbrand, C.-D., & Kuhn, G. (2014). Neodymium and hafnium boundary contributions to seawater along the West Antarctic continental margin. *Earth and Planetary Science Letters*, *394*, 99–110. https://doi.org/10.1016/j.epsl.2014.03.008

Roberts, A. P., Bicknell, S. J., Byatt, J., Bohaty, S. M., Florindo, F., & Harwood, D. M. (2003). Magnetostratigraphic calibration of Southern Ocean diatom datums from the Eocene–Oligocene of Kerguelen Plateau (Ocean Drilling Program Sites 744 and 748). *Palaeogeography, Palaeoclimatology, Palaeoecology*, *198*(1-2), 145–168. https://doi.org/10.1016/S0031-0182(03)00397-3

Roquet, F., Park, Y.-H., Guinet, C., Bailleul, F., & Charrassin, J.-B. (2009). Observations of the fawn trough current over the Kerguelen plateau from instrumented elephant seals. *Journal of Marine Systems*, *78*(3), 377–393. https://doi.org/10.1016/j.jmarsys.2008.11.017

Roy, M., van de Flierdt, T., Hemming, S. R., & Goldstein, S. L. (2007). $^{40}Ar/^{39}Ar$ ages of hornblende grains and bulk Sm/Nd isotopes of circum-Antarctic glacio-marine sediments: Implications for sediment provenance in the southern ocean. *Chemical Geology*, *244*(3-4), 507–519. https://doi.org/10.1016/j.chemgeo.2007.07.017

Salamy, K. A., & Zachos, J. C. (1999). Latest Eocene–early Oligocene climate change and Southern Ocean fertility: Inferences from sediment accumulation and stable isotope data. *Palaeogeography, Palaeoclimatology, Palaeoecology*, *145*(1-3), 61–77. https://doi.org/10.1016/S0031-0182(98)00093-5

Sandwell, D. T., Müller, R. D., Smith, W. H., Garcia, E., & Francis, R. (2014). New global marine gravity model from CryoSat-2 and Jason-1 reveals buried tectonic structure. *Science*, *346*(6205), 65–67. https://doi.org/10.1126/science.1258213

Scher, H. D., Bohaty, S. M., Smith, B. W., & Munn, G. H. (2014). Isotopic interrogation of a suspected late Eocene glaciation. *Paleoceanography*, *29*, 628–644. https://doi.org/10.1002/2014PA002648
Scher, H. D., Bohaty, S. M., Zachos, J. C., & Delaney, M. L. (2011). Two-stepping into the icehouse: East Antarctic weathering during progressive ice-sheet expansion at the Eocene–Oligocene transition. *Geology*, *39*(4), 383–386. https://doi.org/10.1130/G31726.1
Scher, H. D., & Delaney, M. L. (2010). Breaking the glass ceiling for high resolution Nd isotope records in early Cenozoic paleoceanography. *Chemical Geology*, *269*(3-4), 329–338. https://doi.org/10.1016/j.chemgeo.2009.10.007
Scher, H. D., & Martin, E. E. (2004). Circulation in the Southern Ocean during the Paleogene inferred from neodymium isotopes. *Earth and Planetary Science Letters*, *228*(3-4), 391–405. https://doi.org/10.1016/j.epsl.2004.10.016
Scher, H. D., & Martin, E. E. (2006). Timing and climatic consequences of the opening of drake passage. *Science*, *312*(5772), 428–430. https://doi.org/10.1126/science.1120044
Scher, H. D., & Martin, E. E. (2008). Oligocene deep water export from the North Atlantic and the development of the Antarctic circumpolar current examined with neodymium isotopes. *Paleoceanography*, *23*, PA1205. https://doi.org/10.1029/2006PA001400
Scher, H. D., Whittaker, J. M., Williams, S. E., Latimer, J. C., Kordesch, W. E., & Delaney, M. L. (2015). Onset of Antarctic Circumpolar Current 30 million years ago as Tasmanian Gateway aligned with westerlies. *Nature*, *523*(7562), 580–583. https://doi.org/10.1038/nature14598
Seton, M., Müller, R., Zahirovic, S., Gaina, C., Torsvik, T., Shephard, G., … Maus, S. (2012). Global continental and ocean basin reconstructions since 200 Ma. *Earth-Science Reviews*, *113*(3-4), 212–270. https://doi.org/10.1016/j.earscirev.2012.03.002
Smith, N. R., Zhaoqian, D., Kerry, K. R., & Wright, S. (1984). Water masses and circulation in the region of Prydz Bay, Antarctica. *Deep-Sea Research*, *31*(9), 1121–1147. https://doi.org/10.1016/0198-0149(84)90016-5
Sokolov, S., & Rintoul, S. R. (2009). Circumpolar structure and distribution of the Antarctic Circumpolar Current fronts: 1. Mean circumpolar paths. *Journal of Geophysical Research*, *114*, C11018. https://doi.org/10.1029/2008JC005108
Stagg, H. M. J. (1985). The structure and origin of Prydz Bay and MacRobertson Shelf, East Antarctica. *Tectonophysics*, *144*, 315–340.
Staudigel, H., Doyle, P., & Zindler, A. (1985). Sr and Nd isotope systematics in fish teeth. *Earth and Planetary Science Letters*, *76*(1-2), 45–56. https://doi.org/10.1016/0012-821X(85)90147-5
Stein, C. A., & Stein, S. (1992). A model for the global variation in oceanic depth and heat flow with lithospheric age. *Nature*, *359*(6391), 123–129. https://doi.org/10.1038/359123a0
Stichel, T., Frank, M., Rickli, J., & Haley, B. A. (2012). The hafnium and neodymium isotope composition of seawater in the Atlantic sector of the Southern Ocean. *Earth and Planetary Science Letters*, *317*, 282–294.
Stickley, C. E., Brinkhuis, H., Schellenberg, S. A., Sluijs, A., Röhl, U., Fuller, M., … Williams, G. L. (2004). Timing and nature of the deepening of the Tasmanian gateway. *Paleoceanography*, *19*, PA4027. https://doi.org/10.1029/2004PA001022
Strand, K., Passchier, S., & Näsi, J. (2003). Implications of quartz grain microtextures for onset Eocene/Oligocene glaciation in Prydz Bay, ODP Site 1166, Antarctica. *Palaeogeography, Palaeoclimatology, Palaeoecology*, *198*(1-2), 101–111. https://doi.org/10.1016/S0031-0182(03)00396-1
Sykes, T. J. (1996). A correction for sediment load upon the ocean floor: Uniform versus varying sediment density estimations—Implications for isostatic correction. *Marine Geology*, *133*(1-2), 35–49. https://doi.org/10.1016/0025-3227(96)00016-3
Tachikawa, K., Athias, V., & Jeandel, C. (2003). Neodymium budget in the modern ocean and paleo-oceanographic implications. *Journal of Geophysical Research*, *108*(C8), 3254. https://doi.org/10.1029/1999JC000285
Thomas, D. J., Bralower, T. J., & Jones, C. E. (2003). Neodymium isotopic reconstruction of late Paleocene–early Eocene thermohaline circulation. *Earth and Planetary Science Letters*, *209*(3-4), 309–322. https://doi.org/10.1016/S0012-821X(03)00096-7
Thomas, D. J., Korty, R., Huber, M., Schubert, J. A., & Haines, B. (2014). Nd isotopic structure of the Pacific Ocean 70–30 Ma and numerical evidence for vigorous ocean circulation and ocean heat transport in a greenhouse world. *Paleoceanography*, *29*, 454–469. https://doi.org/10.1002/2013PA002535
Torsvik, T. H., Van der Voo, R., Preeden, U., Mac Niocaill, C., Steinberger, B., Doubrovine, P. V., … Tohver, E. (2012). Phanerozoic polar wander, palaeogeography and dynamics. *Earth-Science Reviews*, *114*(3-4), 325–368. https://doi.org/10.1016/j.earscirev.2012.06.007
van de Flierdt, T., Robinson, L. F., Adkins, J. F., Hemming, S. R., & Goldstein, S. L. (2006). Temporal stability of the neodymium isotope signature of the Holocene to glacial North Atlantic. *Paleoceanography*, *21*, PA4102. https://doi.org/10.1029/2006PA001294
van Hinsbergen, D. J., de Groot, L. V., van Schaik, S. J., Spakman, W., Bijl, P. K., Sluijs, A., … Brinkhuis, H. (2015). A paleolatitude calculator for paleoclimate studies (model version 2.0). *PLoS One*, *10*(6), e0126946. https://doi.org/10.1371/journal.pone.0126946
Via, R. K., & Thomas, D. J. (2006). Evolution of Atlantic thermohaline circulation: Early Oligocene onset of deep-water production in the North Atlantic. *Geology*, *34*(6), 441–444. https://doi.org/10.1130/G22545.1
Wallace, P. J. (2002). Volatiles in submarine basaltic glasses from the Northern Kerguelen Plateau (ODP Site 1140): Implications for source region compositions, magmatic processes, and plateau subsidence. *Journal of Petrology*, *43*(7), 1311–1326. https://doi.org/10.1093/petrology/43.7.1311
Weis, D., Frey, F. A., Schlich, R., Schaming, M., Montigny, R., Damasceno, D., … Scoates, J. S. (2002). Trace of the Kerguelen mantle plume: Evidence from seamounts between the Kerguelen Archipelago and Heard Island, Indian Ocean. *Geochemistry, Geophysics, Geosystems*, *3*(6), 1033. https://doi.org/10.1029/2001GC000251
Whittaker, J. M., Afonso, J., Masterton, S., Müller, R., Wessel, P., Williams, S., & Seton, M. (2015). Long-term interaction between mid-ocean ridges and mantle plumes. *Nature Geoscience*, *8*(6), 479–483. https://doi.org/10.1038/ngeo2437
Williams, G. D., Herraiz-Borreguero, L., Roquet, F., Tamura, T., Ohshima, K. I., Fukamachi, Y., … Hindell, M. (2016). The suppression of Antarctic bottom water formation by melting ice shelves in Prydz Bay. *Nature Communications*, *7*, 12577. https://doi.org/10.1038/ncomms12577
Wilson, D. S., & Luyendyk, B. P. (2009). West Antarctic paleotopography estimated at the Eocene-Oligocene climate transition. *Geophysical Research Letters*, *36*, L16302. https://doi.org/10.1029/2009GL039297
Yabuki, T., Suga, T., Hanwa, K., Matsuoka, K., Kiwada, H., & Watanabe, T. (2006). Possible source of the Antarctic Bottom Water in the Prydz Bay region. *Journal of Oceanography*, *62*(5), 649–655. https://doi.org/10.1007/s10872-006-0083-1
Zachos, J. C., Berggren, W. A., Aubry, M.-P., & Mackensen, A. (1992). Isotope and trace element geochemistry of Eocene and Oligocene foraminifers from Site 748, Kerguelen Plateau. In S. W. Wise, Jr., et al. (Eds.), *Proceedings of the Ocean Drilling Program, Scientific Results* (Vol. 120, pp. 839–854). College Station, TX: Texas A&M University. https://doi.org/10.2973/odp.proc.sr.120.183.1992
Zachos, J. C., Breza, J. R., & Wise, S. W. (1992). Early Oligocene ice-sheet expansion on Antarctica: Stable isotope and sedimentological evidence from Kerguelen Plateau, southern Indian Ocean. *Geology*, *20*(6), 569–573. https://doi.org/10.1130/0091-7613(1992)020%3C0569:EOISEO%3E2.3.CO;2
Zachos, J., Pagani, M., Sloan, L., Thomas, E., & Billups, K. (2001). Trends, rhythms, and aberrations in global climate 65 Ma to present. *Science*, *292*(5517), 686–693. https://doi.org/10.1126/science.1059412
Zachos, J. C., Quinn, T. M., & Salamy, K. A. (1996). High-resolution (10^4 years) deep-sea foraminiferal stable isotope records of the Eocene-Oligocene climate transition. *Paleoceanography*, *11*, 251–266. https://doi.org/10.1029/96PA00571